

A SHIFT TECHNIQUE FOR MULTI-PASS WELDING SIMULATION

P. PEREIRA ALVAREZ^{***}, T. DINH TRONG^{**}, S. HENDILI^{*},
V. ROBIN^{*} and J. DELMAS^{*}

^{}EDF R&D, Chatou, France*

*^{**}MINES ParisTech, Centre des matériaux, CNRS UMR 7633, Evry, France pablo.pereira_alvarez@mines-paristech.fr*

DOI 10.3217/978-3-85125-615-4-17

ABSTRACT

The simulation of complex industrial welding processes using the Finite Elements method is not usually feasible within a reasonable time limit due to the strong non linearities of the physical models and the dimensions of the problem. To study many of these industrial cases, we would like to apply simplified methods to compute the simulations in acceptable time. We propose a simplified method called Physical Fields Shift which allows us to accelerate the computations and obtain an approximation of the strain and residual stress state at the scale of the component after the repair process. This method has been applied to an overlay welding repair with successful results.

Keywords: multi-pass welding, shift technique, overlay welding repair

INTRODUCTION

The numerical simulation of welding processes is an extremely complex problem because of the strong non linearities of the physical models and their large spatio-temporal dimensions. In some industrial cases of welding repair, a large number of passes is involved. This large number of passes implies an even greater time expense and thus their study through simulations is almost impossible to achieve in an industrial context. An example of this type of problem is the simulation of a welding repair process called overlay. In this kind of process, more than a hundred passes over two different layers of weld beads are required. Bearing in mind that the simulation of a single pass takes around 10 hours, we immediately realize that the simulation of the whole process using the classical Finite Elements method is not feasible in a reasonable time.

A simplified method called the Physical Fields Shift is proposed. Firstly the Physical Fields Shift method will be explained. Then, we will present a welding procedure that is being studied through numerical simulation: an overlay repair operation. In that section, the parameters of the reference procedure and the consequences of it are discussed. The goal of the following section is to explain the physical models employed in the simulation of an overlay repair, focusing on the mechanical behavior. Finally the performance of both

Mathematical Modelling of Weld Phenomena 12

methods (the proposed Physical Fields Shift method and the classical Finite Elements method) will be compared to empirical data obtained from an industrial overlay procedure.

PHYSICAL FIELDS SHIFT

In the context of one of EDF's research projects on welding, numerical simulation is used as a way to study the thermo-mechanical consequences of many different welding repair processes. These multi-pass simulations usually involve a large number of welding beads arranged in several layers of them. The computation time increases at least quadratically with the number of beads and thus the whole simulation of the welding procedure is not feasible in a reasonable time. To overcome this problem, we propose a simplified method called Physical Fields Shift which allows us to accelerate the computations and obtain an approximation of the strain and residual stress state at the scale of the component after the repair process.

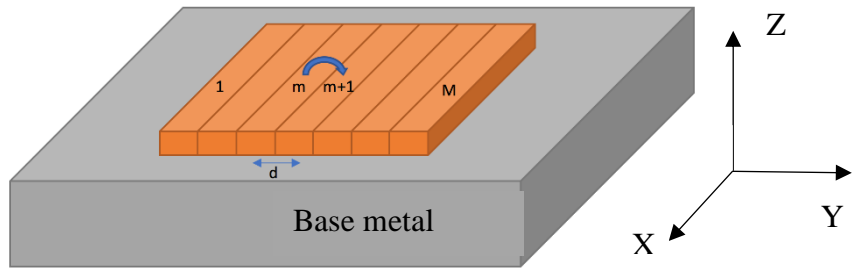


Fig. 1 Schema showing a multi-pass welding toy case (one layer).

The Physical Fields Shift method is based on the similarities observed between two consecutive passes. After a certain number of simulated passes, we observe a propagation of the solution in the sense of the deposit of welding beads. In fact, after each pass, the main difference between two consecutive passes is a spatial translation. Indeed, on the new bead almost the same fields reappear and on the previous beads, the stress and strain accumulate. This evolution will be capitalized to obtain an approximation of the next passes. However, a reasonable number of beads must be computed before applying the method because this observation is not valid on the first beads. Fig. 2 and Fig. 3 show these phenomena in a welding test case consisting of a base metal and 20 welding beads similar to the one in Fig. 1. The curves are plotted over a line that goes from one end of the base to the other, crossing the welding area at the center. A zoom is made on the welding area. The first bead is placed at 60 mm from the end of the plate and is 4 mm large. The last one is placed at 136 mm. In the figures, the tenth bead starts at a 100 mm and the thirteenth starts at 112 mm.

Let $M \in \mathbb{N}$ be the total number of passes. In order to use the method, we need to compute the first m passes by the Finite Elements method, with $m < M$. The objective of the first step is to obtain an approximation of the final state of the $(m+1)^{th}$ pass using the solutions of the m and $m-1$ passes. We assume that the difference between the displacement and stress

Mathematical Modelling of Weld Phenomena 12

fields of the $m+1$ and m passes is going to be similar to that of the m and $m-1$ passes. Let \mathbf{s}_m and \mathbf{s}_{m-1} be the fields representing the final state after the simulation of the $m+1$ and m passes respectively. The first step of the method is to compute a field $\Delta\mathbf{s}_m$ containing the difference between the m and $m-1$ passes. This field is called the increment field and it represents the evolution of displacement and stress from the $m-1$ pass to the m and it is computed as follows:

$$\Delta\mathbf{s}_m = \mathbf{s}_m - \mathbf{s}_{m-1}$$

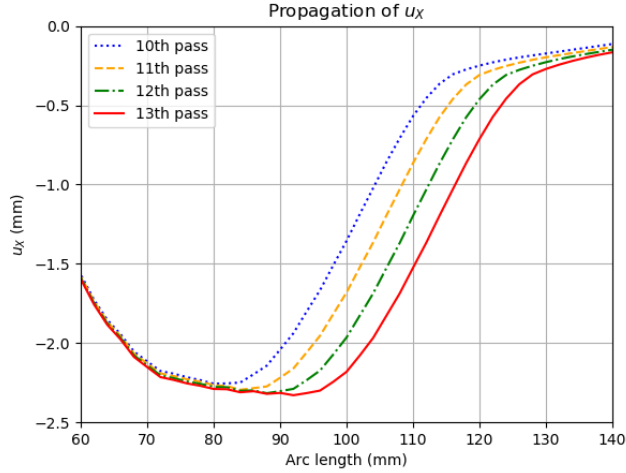


Fig. 2 Final state of displacement of four consecutive passes (X component).

When the increment field is calculated, we need to shift it of a distance d in the direction of the deposit of welding beads. This distance d represents the distance between two beads as shown in Fig. 1. The shifted increment field $\Delta\hat{\mathbf{s}}_m$ approximates the evolution that will happen between the m and $m+1$ passes. Finally, the shifted increment field is used to obtain an approximation $\tilde{\mathbf{s}}_{m+1}$ of \mathbf{s}_{m+1} :

$$\tilde{\mathbf{s}}_{m+1} = \mathbf{s}_m + \Delta\hat{\mathbf{s}}_m$$

Mathematical Modelling of Weld Phenomena 12

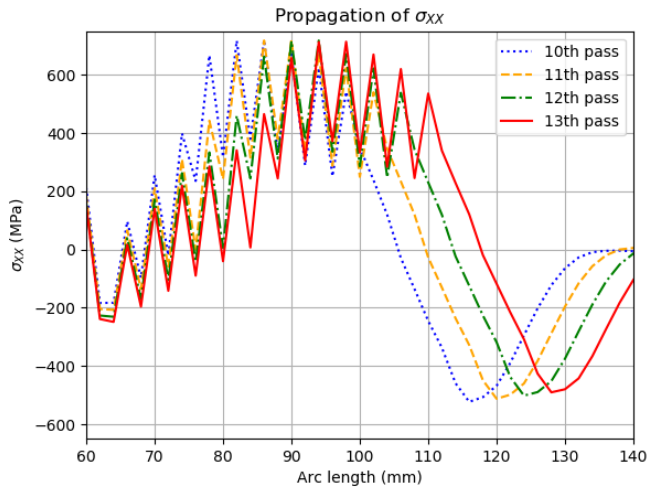


Fig. 3 Final state of longitudinal stresses of four consecutive passes.

The method is applied successively until all of the beads are done. The predictions are accurate in the welding area (see Fig. 4), but not so much outside of it after applying the method many consecutive times. The final step, once all the passes are done, consists in using the predictions as input on the welding area for an elastoplastic re-equilibrium to obtain an approximation of the final state of the physical fields on the whole structure.

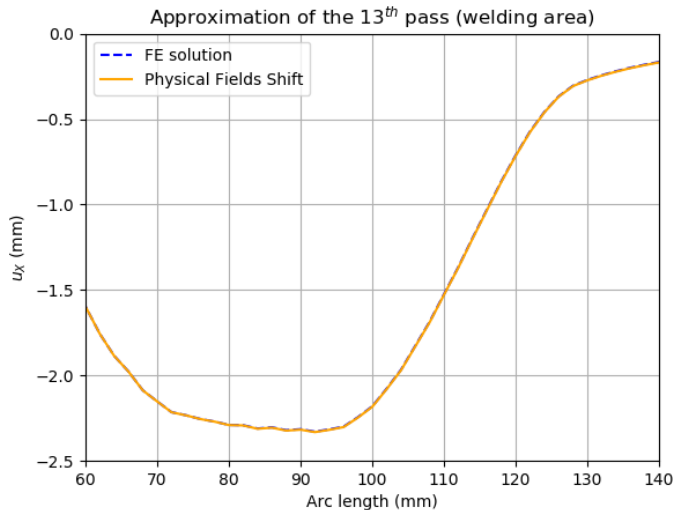


Fig. 4 Approximation of the displacement of the 13th pass (X component).

OVERLAY WELDING REPAIR

Pipes in nuclear power plants sometimes have a thickness defect which could be caused during its fabrication or by erosion. When this kind of defect is detected, it needs to be

Mathematical Modelling of Weld Phenomena 12

repaired using a method called overlay to ensure their mechanical resistance. This technique consists in covering the defected area with one or more layers of welding beads in order to achieve a physical and mechanical continuity. We differentiate between partial overlay, when only a section of the circumference is welded and complete overlay, when the whole circumference is welded. Only the partial overlay is being considered as an example of an industrial case in this document.

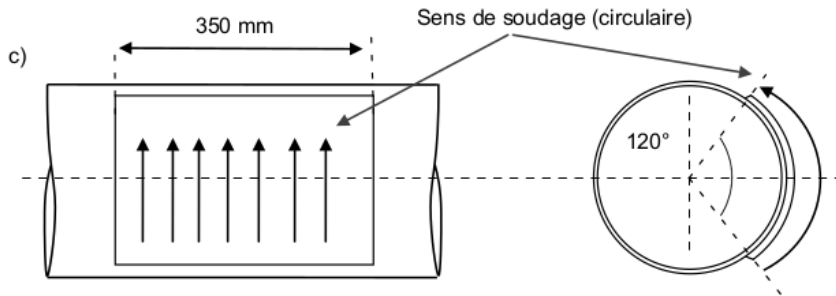


Fig. 5 Schema of the welding area.

The pipe on which the procedure is performed is made from P265GH Schedule 80S steel. It is 1900 mm long, its external diameter is 323.8 mm and its thickness is 12.7 mm. After the operation, we will have a deposition with a thickness of 5.6 mm. A first layer of 3.4 mm and a second one of 2.2 mm. The welding beads are deposited on an area of 350 mm and 120° of the circumference, as shown in the schema in Fig. 5. The welding parameters of the operation are shown in Table 1.

At the end of the procedure, three different types of deformation on the pipe will be observed. Due to the suffered stress during the welding the pipe will bend, changing the angle between the extremities of the pipe. Furthermore, the pipe is deformed at the welding area and its internal diameter is reduced.

Mathematical Modelling of Weld Phenomena 12

Table 1 Welding parameters of the reference experiment.

Parameters	First layer	Second layer
Intensity (A)	193	182
Tension (V)	17,8	17,8
Speed ($cm \cdot min^{-1}$)	13	12
Maximum inter-pass temperature ($^{\circ}C$)	250	250
Energy ($KJ \cdot min^{-1}$)	15,9	16,1
Number of passes	114	91

NUMERICAL MODEL

To simulate a welding procedure, a thermo-mechanical problem is solved using the Finite Elements method with code `_aster`, EDF's Finite Elements software[1]. The pipe is modeled by a 1900 mm cylinder with an external diameter of 323.8 mm and a thickness of 12.7 mm. The welding beads are modeled as a volume 5.6 mm thick covering an area of 120 ° and 350 mm placed in the middle of the pipe. This volume is divided in two layers of 3.4 mm and 2.2 mm respectively. Each layer will be partitioned in a 100 sub-layers in the transverse sense of welding. These sub-layers will represent the welding beads. The pipe and the welding beads are meshed using quadrangular linear elements. The mesh is more refined in the welding area and has a total of 345842 elements. A screenshot of the mesh can be found in the first appendix.

The thermo-mechanical problem is solved in two steps. We first solve the thermal problem and then use the solution as input data for the mechanical problem. The heat problem consists of the classical heat equation in which the heat source is represented as an equivalent heat source using a Goldak function [2]. The other boundary conditions are the heat exchange with the surrounding air (supposed to be at 20°C) and radiation. Table 2 shows the parameters used to solve the heat problem.

The mechanical behavior is supposed to be thermo-elasto-plastic. The thermo-elastic behavior is determined by Young's modulus, Poisson's coefficient and the coefficient of thermal expansion whilst the plastic behavior is described by the von Mises yield criterion and isotropic non-linear hardening. The hardening function $R(p, T)$, dependent on the plastic strain (p) and temperature (T), is computed from stress-strain curves $\sigma(\varepsilon, T)$ obtained from experimental measures. In the third appendix an example of the stress-strain curves for various temperature values are given. The mechanical evolution is produced by the temperature gradients calculated during the resolution of the heat problem. Three points are fixed on one side of the pipe, enough to avoid rigid body movements.

The values of the physical parameters used in the numerical models are shown in the second appendix.

Mathematical Modelling of Weld Phenomena 12

Table 2 Parameters of the heat problem.

Parameters	Values
Heat source's length	10 mm
Efficiency of the heat source	0.55
Heat source speed	13/6 mm · s ⁻¹
Convective transfer coefficient	20 W · m ⁻² · K ⁻¹
Emissivity	0.8
Boltzmann constant	5.67 · 10 ⁻⁸ W · m ⁻² · K ⁻⁴

RESULTS

The goal of this section is to compare the performance of the Physical Fields Shift method to the classical Finite Elements method. To do so, we will compare the computation time of each method and the error between the obtained solution and a reference solution, in this case the experimental data. The computation of the Finite Elements method takes a really long time, so only the first layer of beads is simulated. This method has already been tested with success on an overlay welding procedure in [3].

To apply the Physical Fields Shift method, the twenty first passes are simulated using the Finite Elements method. The choice of twenty beads is done to be sure that the quasi-steady state is achieved. The final instant of the solutions of the 19th and 20th passes are used to approximate the final instant of the 21st pass. Then, the final instant of the 22nd is computed from the final state of the 20th pass and the approximation of the 21st pass. The final state of the rest of the passes are calculated in the same way using the approximations. After the final pass is finished, a quick elastoplastic re-equilibrium is computed introducing the predicted stress and strain fields as imposed values on the welding area to calculate the final strain on the whole pipe.

Mathematical Modelling of Weld Phenomena 12

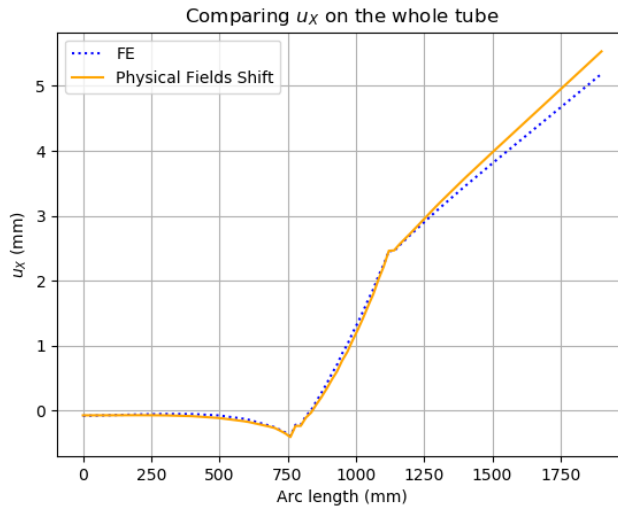


Fig. 6 Comparison of the final state of displacement computed using the Finite Elements method and the Physical Fields Shift method applied 80 times (X component).

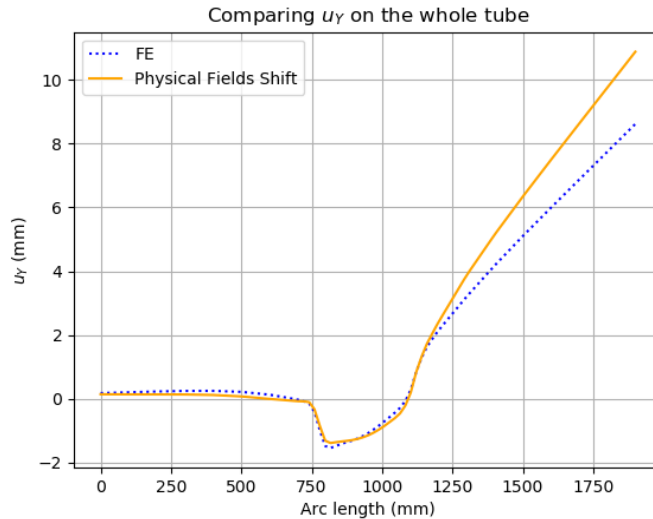


Fig. 7 Comparison of the final state of displacement computed using the Finite Element method and the Physical Fields Shift method applied 80 times (Y component).

The computation time of the Finite Elements simulation is, on average, 2 hours per pass for the heat problem and 7 hours per pass for the mechanical problem. The CPU execution time of the Physical Fields Shift method is 13 seconds per pass on average. The Table 3 allows to compare the time needed to study the welding of the first layer using the Finite Elements method and the Physical Fields Shift method on the last 80 passes.

Mathematical Modelling of Weld Phenomena 12

Table 3 Computation times.

Method	Heat problem	Mechanical problem	Complete problem
Finite Elements	200h	700h	~ 37 days
Physical Fields Shift	40h	140h + 18min	~ 7 days

As it can be observed, around 30 days of computations are saved if only the first 20 passes are computed and then the Physical Fields Shift method is applied. That is effectively 5 times quicker than using the Finite Elements method to compute the total number of welding beads. This gain time may be the difference between a study that can be carried out and one that is impossible to do in an industrial context. These computation times could be further improved reducing the number of passes that are simulated before the first use of the Physical Fields Shift method.

One of the important measures taken during overlay welding is the bending angle of the pipe after the welding. To measure this value, only the displacement fields are necessary. The displacement values at the end of the simulation are shown on Fig. 6 (X component) and Fig. 7 (Y component). In both cases, the Physical Fields Shift method overestimates the values obtained using the Finite Elements method. Those values are plotted over a line going from one end of the tube to the other one. The first bead is placed at 775 mm from the end of the tube. We will now compare the bending angles that we calculated using the Finite Elements method and the Physical Fields Shift method. The Y component of the displacement on one extremity of the pipe is used to compute the arctangent of $Y/(L/2)$ where L is the length of the pipe. Both of those results, as well as the data obtained during the procedure, are shown in Table 4.

Table 4 Bending angles (in degrees).

Method	Experimental data	Finite Elements	Physical Fields Shift
Bending angle	0.537	0.56	0.697

In this case, both methods overestimate the bending angle of the experimental data. We need to bear in mind that the computation of the angle is very sensitive to small variations to the displacement values. The most important results of the Physical Fields Shift method is the reduction of the computation time.

CONCLUSION AND FUTURE WORK

In the context of the EDF's research projects on welding we are confronted with industrial multi-pass problems that are impossible to solve in reasonable time limits, for instance overlay welding procedures. The complexity of the classical Finite Elements method, the

Mathematical Modelling of Weld Phenomena 12

size of the problems and the huge computation times make most of these studies not feasible.

We have presented a simplified method that allows us to obtain reasonable approximations of the final state of an overlay welding procedure in acceptable time limits. The results prove that computation times are improved and solutions are valid.

In addition to this method, these approximations could be used to build reduced order models to apply the hyper-reduction method [4] to obtain more precise results in still reasonable times. Reduced order models for the first passes could also be built and used for parametric studies. Both of these ideas have already been tested in [3] on simple multipass welding examples, but not yet on industrial cases.

REFERENCES

- [1] EDF: 'Finite elements code aster, Analysis of Structures and Thermomechanics for Studies and Research', www.code-aster.org, 1989–2018.
- [2] J. GOLDAK, A. CHAKRAVARTI, and M. BIBBY: 'A new finite element model for welding heat sources', *Metallurgical and Materials Transactions*, B 15, 2 (1984), 299–305.
- [3] T. DINH TRONG: *Modèles hyper-réduits pour la simulation simplifiée du soudage en substitut de calcul hors d'atteinte*, thesis, Centre des Matériaux, Mines ParisTech, 2018.
- [4] D. RYCKELYNCK: 'A priori hyperreduction method: an adaptive approach', *Journal of computational physics*, 202(1) :346–366, 2005.

APPENDIX 1: MESH USED FOR THE SIMULATIONS

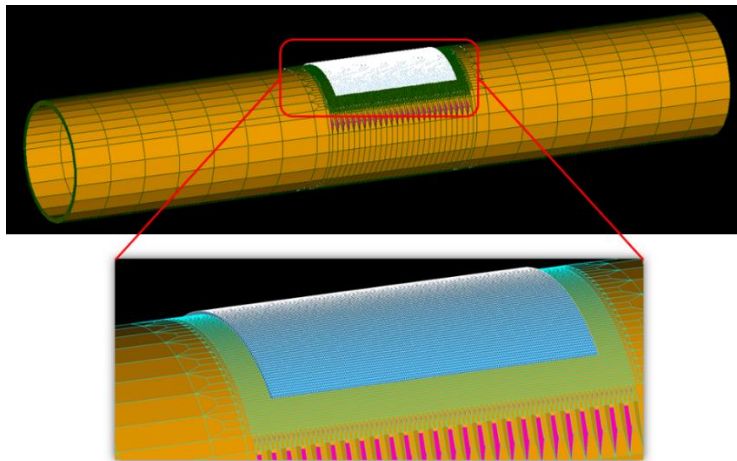


Fig. 8 Mesh used in overlay simulations with zoom on the welding area.

APPENDIX 2: PHYSICAL PARAMETERS FOR THE NUMERICAL MODEL

The following tables include the physical parameters of P265GH Schedule 80S steel:

Mathematical Modelling of Weld Phenomena 12

Table 5 Thermo-physical parameters (temperature dependent).

Temperature (°C)	Thermal conductivity ($W \cdot mm^{-1} \cdot K^{-1}$)	Heat capacity ($J \cdot mm^{-3} \cdot K^{-1}$)
20	4.93E-02	3.71E-03
100	4.83E-02	3.80E-03
200	4.67E-02	3.88E-03
300	4.35E-02	4.02E-03
400	3.98E-02	4.19E-03
500	3.59E-02	4.38E-03
600	3.23E-02	4.58E-03
700	2.88E-02	4.79E-03
800	2.37E-02	5.28E-03
900	2.54E-02	5.22E-03
1000	2.67E-02	5.17E-03
1100	2.80E-02	5.12E-03
1200	2.94E-02	5.06E-03
2200	2.94E-01	5.06E-03

Table 6 Thermo-elastic parameters (temperature dependent).

Temperature (°C)	Young's modulus (MPa)	Coefficient of thermal expansion (°C ⁻¹)	Poisson's coefficient
20	2.12E+05	1.11E-05	0.3
100	2.02E+05	1.15E-05	0.3
200	1.94E+05	1.22E-05	0.3
300	1.88E+05	1.28E-05	0.3
400	1.81E+05	1.33E-05	0.3
500	1.71E+05	1.38E-05	0.3
600	1.59E+05	1.43E-05	0.3
700	1.42E+05	1.49E-05	0.3
800	1.22E+05	1.25E-05	0.3
900	1.00E+05	1.34E-05	0.3
1000	7.92E+04	1.42E-05	0.3
1100	6.24E+04	1.50E-05	0.3
1200	4.91E+04	1.57E-05	0.3

APPENDIX 3: STRESS-STRAIN CURVES FOR THE HARDENING FUNCTION

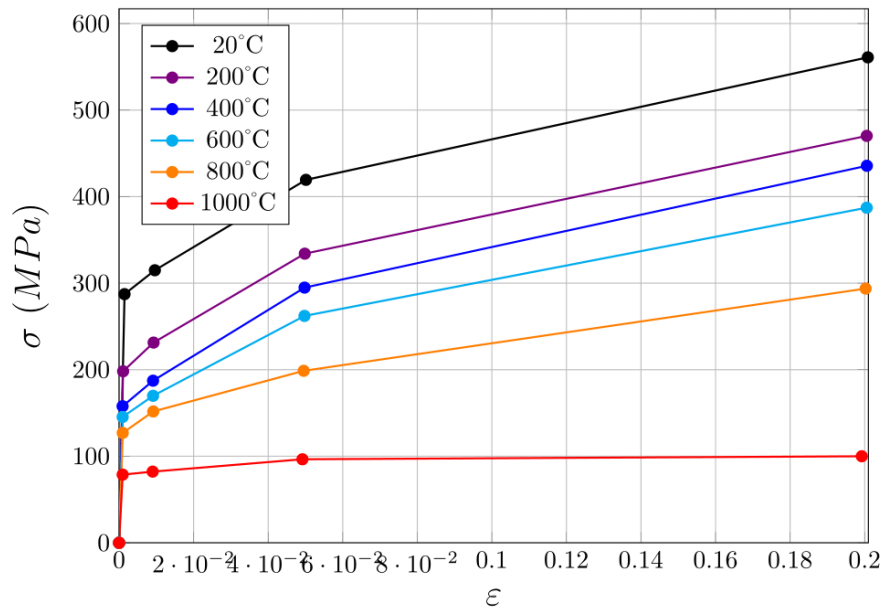


Fig. 9 Stress-strain curves used to compute the hardening function.